Publication I

Pia Myllymäki, Minna Nieminen, Jaakko Niinistö, Matti Putkonen, Kaupo Kukli, and Lauri Niinistö. 2006. High-permittivity $YScO_3$ thin films by atomic layer deposition using two precursor approaches. Journal of Materials Chemistry, volume 16, number 6, pages 563-569.

High-permittivity YScO$_3$ thin films by atomic layer deposition using two precursor approaches

Pia Myllymäki,*[a] Minna Nieminen,[a] Jaakko Niinistö,[a] Matti Putkonen,[a] Kaupo Kukli[bc] and Lauri Niinistö[a]

Amorphous YScO$_3$ thin films have been deposited by atomic layer deposition using two types of volatile metal precursors, *viz.* β-diketonate-type metal complexes M(thd)$_3$ (M = Y, Sc; thd = 2,2,6,6-tetramethyl-3,5-heptanedionato) and organometallic cyclopentadienyl compounds tris(methylcyclopentadienyl)yttrium (C$_5$H$_4$CH$_3$)$_3$Y and tris(cyclopentadienyl)scandium Cp$_3$Sc (Cp = C$_5$H$_5$). Ozone and water were used as oxygen sources in the M(thd)$_3$ and cyclopentadienyl precursor-based processes, respectively. Deposition temperatures were 335–350 °C for the M(thd)$_3$ precursor-based process and 300 °C for the cyclopentadienyl precursor-based process. Metal ratio and film thickness were easily controlled by varying the metal precursor pulsing ratio and the number of deposition cycles. Stoichiometric YScO$_3$ films contained less than 1 atom% hydrogen and less than 0.2 atom% carbon regardless of the precursors used. The as-deposited stoichiometric films were smooth, amorphous and they had high permittivity (14–16). Films deposited using the cyclopentadienyl precursor-based process started to crystallize at 800 °C while films deposited using the M(thd)$_3$ precursor-based process still remained amorphous at this temperature. Films deposited using the latter process crystallized at 1000 °C. Crystallization significantly deteriorated the dielectric properties of the films, however.

Introduction

Rare earth oxides (REOs) are highly desired materials for various applications, especially in microelectronics.[1] Among the REOs, ternary rare earth metal scandates, *e.g.* LaScO$_3$, GdScO$_3$ and DyScO$_3$, have recently gained considerable interest as possible high-*k* gate oxides to replace SiO$_2$ in MOSFETs.[2] In the amorphous state, they possess excellent electrical properties, *e.g.* high permittivity, low leakage current and small hysteresis. Furthermore, they have high band offset with silicon and are thermally stable.[3] GdScO$_3$ and DyScO$_3$ in particular have been found to preserve their amorphous structure even after prolonged thermal annealing at high temperatures.[4] The ionic radius of six-coordinated Y^{3+} (90.0 pm) is similar to the ionic radius of six-coordinated Dy^{3+} (91.2 pm),[5] and therefore similar crystallization behavior of YScO$_3$ and DyScO$_3$ is to be expected. YScO$_3$ thin films have previously been prepared only by physical vapor deposition (PVD) methods, *e.g.* sputtering[6,7] and electron beam evaporation.[8] To the best of our knowledge, chemical vapor deposition (CVD) of YScO$_3$ or deposition by other chemical vapor phase methods have not been studied earlier.

In the Y$_2$O$_3$–Sc$_2$O$_3$ system two crystalline phases are formed: YScO$_3$ having distorted perovskite structure and Y$_3$ScO$_6$ with rhombohedral structure.[9] The perovskite structure of YScO$_3$ is thermodynamically stable at temperatures below 1700 °C.[9] However, several hours of annealing at high temperature[10] or under high pressure[11] is needed to synthesize the perovskite compound. The rhombohedral Y$_3$ScO$_6$, on the other hand, is stable at temperatures below 1600 °C.[9] At temperatures above 1700 °C, the Y$_2$O$_3$–Sc$_2$O$_3$ system forms a continuous series of solid solutions based on the C-type of rare earth oxides.[12] YScO$_3$ thin films prepared by PVD methods have been found to form amorphous solid solutions of Y$_2$O$_3$ and Sc$_2$O$_3$ rather than ternary compounds.[6,8] Nevertheless, the amorphous structure is often beneficial and provides better dielectric properties than the polycrystalline structure. Dielectric constant of 12–17 has been reported for the sputtered YScO$_3$ film with a thickness of 50–1000 nm.[6]

Atomic layer deposition (ALD) is a variant of the well-known CVD method. The ALD method is based on self-limiting surface reactions achieved by alternating surface-saturating precursor doses separated by inert gas purging. The ALD method has been widely used for the deposition of binary metal oxide films, but also more complex multi-component oxides and layered structures have been deposited.[13–16] However, lack of a suitable precursor combination often sets its limitations for ALD process development. In an ideal case, the constituent binary oxide processes have overlapping ALD windows, *i.e.* temperature ranges of constant growth rate. Although in practice this is seldom the case, multi-component films can be deposited as long as the growth of constituent binary oxides is surface-saturated ALD-type growth. Indeed, several multi-component oxide thin

[a]*Laboratory of Inorganic and Analytical Chemistry, Helsinki University of Technology, P. O. Box 6100, FIN-02015 Espoo, Finland. E-mail: Pia.Myllymaki@hut.fi*
[b]*Department of Chemistry, University of Helsinki, P. O. Box 55, FIN-00014 Helsinki, Finland*
[c]*Institute of Experimental Physics and Technology, University of Tartu, Tähe 4, EE-51010 Tartu, Estonia*

films have been successfully deposited by ALD, e.g. yttria-stabilized zirconia (YSZ),[17] $CeO_2–Gd_2O_3$ (CGO),[18] $SrTiO_3$,[19,20] $NdAlO_3$[21] as well as several lanthanum-based oxides, e.g. $LaNiO_3$,[22] $LaAlO_3$,[23] $LaGaO_3$[24] and $LaMnO_3$.[25]

Here we wish to report the results of our investigation into the controlled thin film growth of $Y_xSc_yO_3$ with different metal ratios using β-diketonates $M(thd)_3$ (M = Y, Sc; thd = 2,2,6,6-tetramethyl-3,5-heptanedionato) and organometallic cyclopentadienyl compounds tris(methylcyclopentadienyl)-yttrium $(C_5H_4CH_3)_3Y$ and tris(cyclopentadienyl)scandium Cp_3Sc (Cp = C_5H_5) as precursors in the ALD processes. Self-limiting deposition of binary Sc_2O_3[26] and Y_2O_3[27–30] thin films by ALD using these precursors has been established earlier. In general, $M(thd)_3$ compounds are air-stable and therefore easy to handle. However, the deposition rate using these precursors is generally quite low and a strong oxidizer, viz. ozone, is needed to obtain good quality oxide thin films.[31] On the other hand, cyclopentadienyl-type compounds yield considerably higher deposition rates and water can be used as the oxygen source. They are, however, air-sensitive and therefore more difficult to synthesize and handle. In the present study, in addition to the film deposition by ALD, film composition, crystallinity, surface morphology and electrical properties are also examined.

Experimental

Thin film deposition

$Y_xSc_yO_3$ thin films were deposited in a commercial flow-type hot-wall ALD-reactor (F-120 by ASM Microchemistry Ltd.). $M(thd)_3$ (M = Y, Sc) precursors were prepared by the method described by Eisentraut and Sievers[32] and purified by sublimation. With $M(thd)_3$ as the metal precursor (thd-based process), ozone was used as oxygen source. O_3 was generated from O_2 (99.999%) in an ozone generator (Fischer model 502). $(C_5H_4CH_3)_3Y$ and Cp_3Sc were obtained from the Institute of Organometallic Chemistry, Russian Academy of Sciences (Nizhny Novgorod, Russia). Air and moisture sensitive cyclopentadienyl-compounds were handled in a glovebox and inertly transferred into the reactor. Distilled water was used as oxygen source for the cyclopentadienyl-compounds (Cp-based process). Water was evaporated from a container kept at room temperature. Nitrogen (>99.999%, Schmidlin UHPN 3000 N_2 generator) was used as carrier and purging gas. Thin film depositions were carried out under 2–3 mbar reactor pressure onto Si(100) and soda lime glass substrates. Glass substrates were ultrasonically cleaned in ethanol and water before use. Silicon substrates were used as received without removing the native oxide. Deposition parameters are summarized in Table 1.

Characterization methods

Film thicknesses were determined by optical fitting method as described by Ylilammi and Ranta-aho.[33] In this method, a theoretical spectrum is fitted to a measured optical transmittance or reflectance spectrum. Reflectance spectra (190–1100 nm) for films deposited on Si and transmittance spectra (370–1100 nm) for films on glass were measured in a Hitachi U-2000 double beam spectrophotometer. Thicknesses of samples used in the electrical characterization were also measured by X-ray reflectometry (XRR) using a Bruker D8 Advance X-ray diffractometer.

The crystallinity of thin films was determined by X-ray diffraction using Cu Kα radiation (Philips MPD 1880). Some of the samples were analyzed also after thermal annealing. Annealing was carried out in nitrogen atmosphere for 10 min at temperatures 800 and 1000 °C using a rapid thermal annealing furnace PEO 601 (ATV Technologie GmbH).

The yttrium to scandium ratio in the films was measured by XRF (Philips PW 1480 WDS spectrometer) using Rh excitation. Data were analyzed with the UNIQUANT 4.34 program which utilizes a DJ Kappa model to calculate the composition and mass thickness of an unknown bulk or thin film sample.[34] Selected samples were also analyzed by time-of-flight elastic recoil detection analysis (TOF-ERDA)[35,36] to determine impurities and the metal to oxygen ratio. TOF-ERDA measurements of films deposited using the $M(thd)_3/O_3$-process were carried out at Interuniversity Microelectronics Center, Belgium. A 16 MeV $^{63}Cu^{7+}$ ion beam was used. Films deposited using cyclopentadienyl-compounds were analysed at the Acceleration Laboratory of the University of Helsinki. A beam of $^{127}I^{10+}$ ions at 53 MeV was obtained from a 5 MV tandem accelerator EGP-10-II.

Surface morphology of the films was probed by a Nanoscope III atomic force microscope (Digital Instruments) operated in tapping mode. Samples were measured with a scanning frequency of 1 Hz. Measured scanning area was 2 × 2 μm and roughness values were calculated as root mean square values.

For the electrical characterization, $YScO_3$ films were deposited by the thd- and Cp-based processes onto native SiO_2-covered p-type Si(100)-substrates at 350 and 300 °C, respectively. Films were analyzed before and after thermal annealing at 800 °C (N_2, 10 min). The $YScO_3$ layer thicknesses were around 40 nm. Aluminium gate electrodes with an effective area of 0.204 mm^2 were e-beam-evaporated onto the $YScO_3$ film surface through a shadow mask. The backsides of

Table 1 Deposition parameters for $Y_xSc_yO_3$ thin films

| Precursor	Evaporation temperature/°C	Metal precursor		Oxygen source	Oxygen source		Deposition temperature/°C
		Pulse/s	Purge/s		Pulse/s	Purge/s	
$Y(thd)_3$	125	0.8	1.0	O_3	1.5	2.0	335–350
$Sc(thd)_3$	115	0.8	1.0	O_3	1.5	2.0	335–350
$(C_5H_4CH_3)_3Y$	110	1.0	1.2	H_2O	1.0	1.5	300
Cp_3Sc	140	1.0	1.2	H_2O	1.0	1.5	300

the Si substrates were HF-etched before evaporating the 100 nm thick aluminum electrodes to create ohmic contacts. Thus, the capacitance–voltage (C–V) and current–voltage (I–V) measurements were performed on Al/YScO$_3$/native SiO$_2$/p-Si(100)/Al capacitor structures. C-V characteristics were measured with an HP 4284A precision LCR-meter. The voltage step was 0.05 V and the frequency of the a.c. signal was 500 kHz. The I-V voltage curves were measured with a Keithley 2400 Source Meter using a voltage step of 0.05 V. All measurements for the as-deposited and annealed samples were carried out at room temperature.

Results and discussion

Thin film deposition

Surface-controlled deposition of the binary oxides Y$_2$O$_3$ and Sc$_2$O$_3$ by ALD using M(thd)$_3$-precursors (M = Y, Sc) can be observed in the temperature ranges 250–375 °C and 335–375 °C, respectively.[26,28] Therefore operating the ternary process for Y$_x$Sc$_y$O$_3$ in the temperature range 335–350 °C should be within the ALD window. The reported deposition rates for Y$_2$O$_3$ and Sc$_2$O$_3$ with the thd-precursors at 350 °C are 0.23 and 0.125 Å (cycle)$^{-1}$, respectively.[26,28] In the present study, thin film growth rates were determined as a function of precursor pulsing ratios at two different temperatures, viz. 335 and 350 °C. Number of the deposition cycles was varied in order to achieve the desired film thickness. Using the pulsing ratio Y : Sc = 1 : 1 the growth rate on silicon remained constant (0.18 Å (cycle)$^{-1}$) at both temperatures and independent of the number of deposition cycles, which is characteristic for ALD-type growth. The growth rates are in good accordance with theoretical growth rates calculated from the previously reported binary oxide growth rates[26,28] (Fig. 1). Growth rate obtained on glass with the pulsing ratio Y : Sc = 1 : 1 was only slightly lower, viz. 0.17 Å (cycle)$^{-1}$.

With cyclopentadienyl-compound precursors, Y$_2$O$_3$ and Sc$_2$O$_3$ films have previously been deposited at temperatures 200–400 °C[30] and 250–350 °C,[26] yielding growth rates 1.2–1.3 and 0.75 Å (cycle)$^{-1}$ on silicon. In this study, the
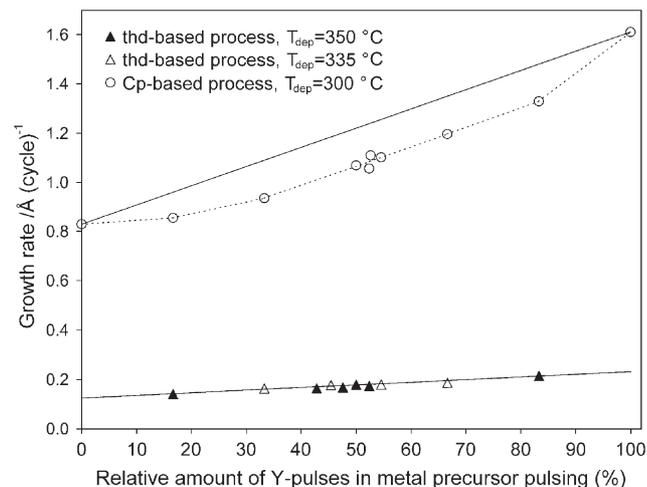
deposition temperature of 300 °C was used for two reasons: Firstly, it is in the middle of the rather wide and overlapping ALD windows for both binary processes, and secondly, impurity levels are low when operating at this temperature.[26,30] Metal pulsing ratio and number of deposition cycles were varied to establish the optimum conditions. Growth rates 1.6 and 0.83 Å (cycle)$^{-1}$ were observed for the binary oxides Y$_2$O$_3$ and Sc$_2$O$_3$, respectively. These values are slightly higher than previously reported growth rates on silicon.[26,30] The growth rate of a film with Y : Sc pulsing ratio of 1 : 1 was 1.07 Å (cycle)$^{-1}$. This growth rate is somewhat lower than the theoretical growth rate calculated from the binary oxide growth rates. Individual pulsing ratios give approximately 10–14% lower growth rates than the theoretical growth rate, as seen in Fig. 1. Similar behavior has also been observed when depositing other ternary rare earth oxides, e.g. LaAlO$_3$[23] and LaGaO$_3$.[24] With a fixed pulsing ratio, however, the process based on cyclopentadienyl-compound precursors gives a linear relationship between the number of deposition cycles and the film thickness. Also in this case the growth rate on glass was slightly lower, viz. 1.01 Å (cycle)$^{-1}$ with the pulsing ratio Y : Sc = 1 : 1.

YScO$_3$ film characteristics

According to XRF analysis, the yttrium to scandium ratio in both processes was nearly linearly dependent on the pulsing ratio (Fig. 2). Therefore it was easy and straightforward to deposit a film with the desired Y : Sc ratio. Using the thd-based process, pulsing ratios Y : Sc = 1 : 1 and 10 : 11 resulted in films with metal ratios Y : Sc = 1.09 and 0.95, respectively, while the stoichiometric ratio is 1.0. With the Cp-based process, pulsing ratios Y : Sc = 1 : 1 and 6 : 5 resulted in films with metal ratios Y : Sc = 0.85 and 1.01, respectively. Films with compositions closest to the stoichiometric, viz. those deposited using pulsing ratios Y : Sc = 10 : 11 and 6 : 5 with the thd- and Cp-based processes, respectively, were investigated in more detail by TOF-ERDA (Table 2).

According to the TOF-ERDA results, films deposited by both processes had low impurity contents. Ternary YScO$_3$ thin films contained less than 1 atom% hydrogen regardless of the

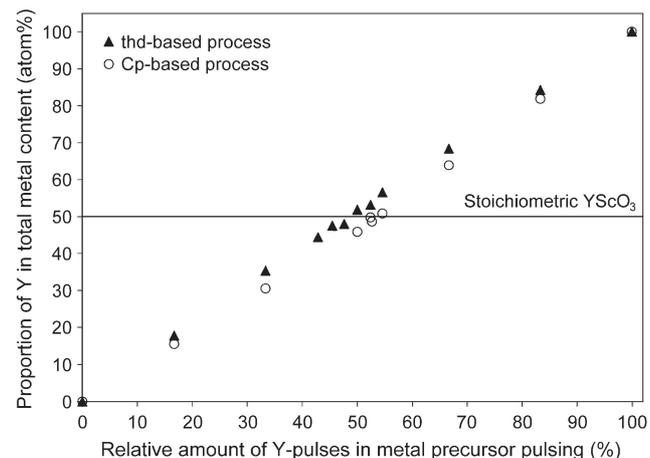

Fig. 1 Measured Y$_x$Sc$_y$O$_3$ film growth rates and the theoretical growth rates (solid lines) as a function of the Y precursor pulsing.

Fig. 2 Relative amount of Y in the total metal content of the films according to XRF analysis.

This journal is © The Royal Society of Chemistry 2006

J. Mater. Chem., 2006, **16**, 563–569 | 565

Table 2 Impurities, metal to oxygen ratio and film composition according to TOF-ERDA

	$M(thd)_3 + O_3$ process	Cp-compound + H_2O process
Y (atom%)	18 ± 2	20.4 ± 0.5
Sc (atom%)	22 ± 2	19.1 ± 0.5
O (atom%)	58 ± 3	59.7 ± 1.0
H (atom%)	0.7 ± 0.2	0.8 ± 0.2
C (atom%)	<0.2	0.1 ± 0.1
F (atom%)	0.9 ± 0.1	—
M/O	0.69	0.66
Pulsing ratio Y : Sc	10 : 11	6 : 5
Composition	$Y_{0.92}Sc_{1.12}O_{2.96}$	$Y_{1.03}Sc_{0.96}O_{3.01}$

precursors used. Carbon content in films was also very low (<0.2 atom%) with both processes. Binary Y_2O_3 thin films studied earlier had contained 1.3–3.1 atom% hydrogen and 1.4–0.2 atom% carbon depending on the precursor used.[28,30] On the other hand, binary Sc_2O_3 films studied earlier showed only small amounts of hydrogen (0.5–0.1 atom%) and carbon (<0.1 atom%) as impurities.[26] Furthermore, small concentration of fluorine was detected in the $YScO_3$ films deposited by the thd-based process. Fluorine has also been detected in binary Y_2O_3 and Sc_2O_3 thin films when ozone has been used as the oxygen source.[26,28] Fluorine is believed to originate from the Teflon gaskets or perfluorinated vacuum greases used in the reactor when in contact with O_3. In the films deposited by the Cp-based process without ozone, no fluorine was detected. Metal to oxygen ratios were M/O = 0.69 and 0.66 with the thd- and Cp-based processes, respectively, while the stoichiometric ratio is 0.67.

According to XRD, most of the as-deposited films on silicon were amorphous. With the thd-based process, films deposited using pulsing ratios Y : Sc = 10 : 1 and 1 : 10 and having metal ratios Y : Sc = 10.3 and 0.11, respectively, were polycrystalline. Films with compositions closer to stoichiometric $YScO_3$ were all amorphous. They remained amorphous after annealing at 800 °C in N_2 atmosphere but began to crystallize during a 10 min annealing at 1000 °C (Fig. 3). The d-values of diffraction peaks shifted as a function of the film composition, as can be seen in the inset of Fig. 3. This indicates that thermally treated films consisted of solid solutions of cubic Y_2O_3 and Sc_2O_3. This behavior is not unexpected, since the Y_2O_3–Sc_2O_3-system is known to form a continuous series of solid solutions based on the C-type of rare earth oxides.[9] The as-deposited films on glass showed similar crystallization behavior as those deposited on silicon with two exceptions. Crystalline structure was observed when pulsing ratios Y : Sc = 5 : 1 and 1 : 5 were used, giving metal ratios Y : Sc = 5.34 and 0.22, respectively. Also when the film thickness exceeded 220 nm, the nearly stoichiometric $YScO_3$ films on glass substrates partly crystallized. Reason for this crystallization behavior remained unclear.
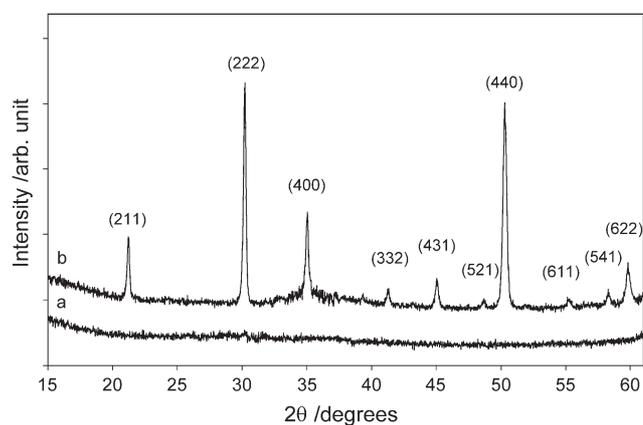
With the Cp-based process pulsing ratios Y : Sc = 5 : 1 and 1 : 5, the ALD depositions yielded polycrystalline films with metal ratios Y : Sc = 4.52 and 0.18, respectively. Also in this case the as-deposited films with composition close to the stoichiometric $YScO_3$ were amorphous. Films started to crystallize during a 10 min annealing at 800 °C (Fig. 4).
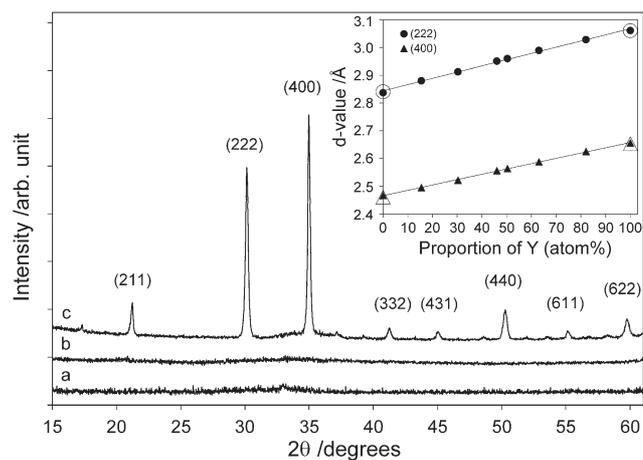

Fig. 3 Diffraction patterns of $YScO_3$ films deposited by the thd-based process using the pulsing ratio of Y : Sc = 1 : 1, which yielded the metal ratio Y : Sc = 1.09. The as-deposited film (a) and the film annealed at 800 °C (b) are amorphous while the film annealed at 1000 °C (c) has a polycrystalline structure. The inset shows a shift of diffraction peak d-values as a function of the film composition. Open symbols represent d-values for Y_2O_3 and Sc_2O_3, used as reference. Diffraction peaks were identified according to JCPDS cards 25–1200 (Y_2O_3) and 5–629 (Sc_2O_3).

Similar shift of the d-values was observed as described above. The as-deposited films on glass substrates showed also similar crystallization behavior as those deposited on silicon.

Surface morphology was studied by atomic force microscopy as a function of the precursor and post-deposition annealing temperatures used. The as-deposited, stoichiometric $YScO_3$ films were smooth and featureless regardless of the process applied. The calculated rms-roughnesses were below 0.5 nm for about 40 nm thick films deposited with both processes. As an example, Fig. 5a shows an AFM image of 44 nm thick $YScO_3$ film deposited by the Cp-based process.
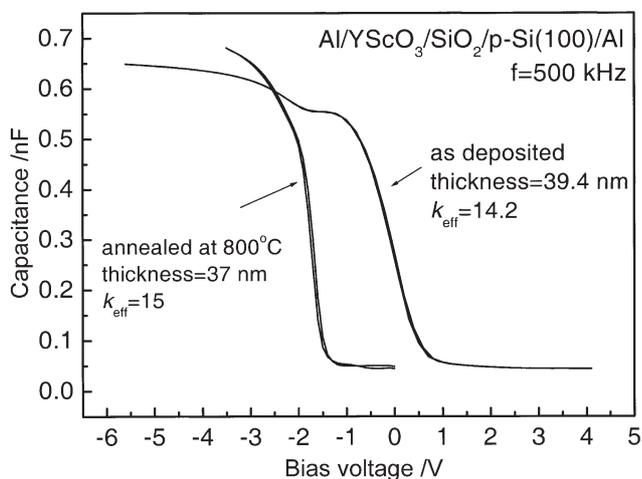

Fig. 4 Diffraction patterns of $YScO_3$ films deposited by the Cp-based process using the pulsing ratio Y : Sc = 6 : 5, which yielded the metal ratio Y : Sc = 1.01. The as-deposited film (a) is amorphous while the film annealed at 800 °C (b) has a polycrystalline structure. Diffraction peaks were identified according to JCPDS cards 25–1200 (Y_2O_3) and 5–629 (Sc_2O_3).
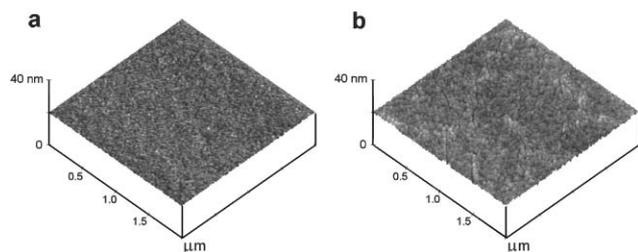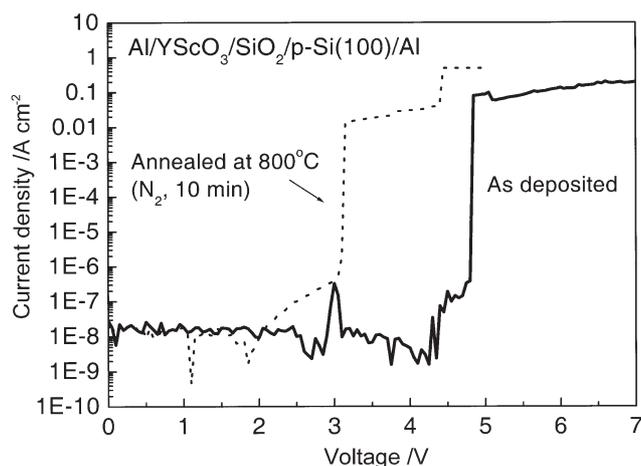
Fig. 5 AFM image of as-deposited YScO₃ film (Cp-based process) (a) and that of an annealed (1000 °C, N₂) film deposited by the thd-based process. (b) The rms-roughness and the film thickness values are 0.4 and 44.1 nm (a) and 0.5 and 37 nm (b), respectively. Image size: 2 × 2 μm. Depth scale: 20 nm from black to white.

As expected, the amorphous structure seems to be beneficial when smooth morphology is desired. Annealing at 800 °C had no effect on the surface roughness of the films regardless of the precursors. However, annealing at 1000 °C produced cracks on the film surface (Fig. 5b).

Fig. 6 shows capacitance–voltage curves for the Al/YScO₃/SiO₂/p-Si(100) capacitor structures where the as-deposited and annealed (800 °C, N₂, 10 min) YScO₃ film was grown using the thd-based process. The flatband voltage shift, often characteristic to ALD-grown rare earth oxide films,[31] is about 1 V towards the positive direction, indicative of fixed charge in the oxide. The annealing changed the shift to the negative direction. The hysteresis was low even for the as-deposited films but a shoulder-like feature was clearly visible. This "hump" or shoulder-like feature can sometimes be observed in high-permittivity oxide–silicon based MOS structures and can be attributed to the interface defects and traps associated with unpassivated silicon dangling bonds.[37] The hump completely disappeared upon annealing. The effective permittivity for the as-deposited 40 nm film was above 14. When compared to the binary oxides Y₂O₃ and Sc₂O₃ deposited by ALD with

Fig. 7 Leakage current density–voltage curves for Al/YScO₃/native SiO₂/p-Si. YScO₃ layer thicknesses: 39.4 nm (as-deposited) and 37 nm (annealed).

thd-precursors and ozone, the effective permittivity was significantly higher; the binary oxides exhibited effective permittivity values of about 9–10. Current–voltage characteristics showed low leakage current densities (1×10^{-8} A cm⁻² at $V_{FB} = 1$ V for 40 nm film) and high breakdown voltages (4–5 V) for the as-deposited films (Fig. 7). An amorphous structure effectively blocks the current from leaking through the dielectric. Annealing slightly decreases the breakdown voltage. Clearly, combining the two binary oxide processes and forming an amorphous ternary YScO₃ phase improves the dielectric properties compared to those of the constituent oxides.

When Cp-based processes were applied, the hysteresis of C–V curve was considerably larger than for the YScO₃ films deposited by the thd-based process (Fig. 8). Hysteresis appearing during the back-forth sweep of capacitance–voltage

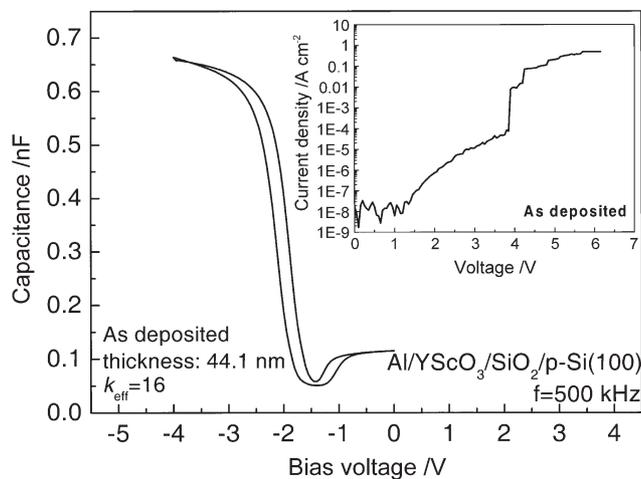**Fig. 6** Capacitance–voltage curves of Al/YScO₃/native SiO₂/p-Si capacitor structures with YScO₃ film grown by the thd-based process. Labels indicate the YScO₃ film thickness, effective permittivity and whether the film is as-deposited or has been annealed at 800 °C (N₂, 10 min).

Fig. 8 Capacitance–voltage curves of Al/YScO₃/native SiO₂/p-Si capacitor structure with YScO₃ film grown by the Cp-based process. Labels indicate the YScO₃ film thickness and effective permittivity. The inset shows the leakage current density–voltage characteristics of the structure.

This journal is © The Royal Society of Chemistry 2006

J. Mater. Chem., 2006, **16**, 563–569 | 567

curves can be taken as a measure of oxide band gap states caused by structural disorder[38] and/or formation of inner-interface defective regions.[39] Since the content of impurities and degree of disorder in the as-deposited states were quite similar for all the films regardless of the precursors, it is not yet unambiguously clear why the capacitors fabricated by the Cp-based process demonstrated larger hysteresis. It is possible that the hysteresis is sensitive to occasional variations in stoichiometry and to microstructural peculiarities as the films deposited by the Cp-based process were more prone to phase separation and re-crystallization upon annealing. Again, the effective permittivity (16) was significantly higher than that (10) obtained for the binary Y_2O_3 grown by the Cp-based ALD process.[30] The inset shows current–voltage characteristics where slightly higher leakage current values are observed as compared to the $YScO_3$ deposited by the thd-based process. As described above, annealing at 800 °C caused the film to crystallize as a solid solution of Y_2O_3 and Sc_2O_3, which led to a significant decrease in effective permittivity, *viz.* reduced it from 16 to about 10. The beneficial effect of having an amorphous ternary oxide is lost upon crystallization induced by annealing because a mixture of lower permittivity binary oxide phases is formed.

Conclusion

$Y_xSc_yO_3$ thin films were deposited from β-diketonates $M(thd)_3$ (M = Y, Sc) and cyclopentadienyl compounds, namely $(C_5H_4CH_3)_3Y$ and Cp_3Sc. Ozone and water were used as oxygen sources in the thd- and Cp-based processes, respectively. Deposition temperatures were 335–350 °C for the thd-based process and slightly lower or 300 °C for the Cp-based process. With the metal precursor pulsing ratio of Y : Sc = 1 : 1, the deposition rate on silicon using thd-compounds was 0.18 Å (cycle)$^{-1}$, while a considerably higher deposition rate of 1.07 Å (cycle)$^{-1}$ was achieved with the Cp-based processes. With both processes, the film composition was easily controlled by varying the metal precursor (Y : Sc) pulsing ratio. The film stoichiometry was maintained while increasing the film thickness, thus verifying the good surface-controlled nature of the processes. Impurity contents were below 1 atom% for hydrogen and less than 0.2 atom% for carbon, regardless of the process used. The as-deposited stoichiometric films were amorphous while polycrystalline solid solutions of C-type cubic Y_2O_3 and Sc_2O_3 were obtained upon thermal annealing at 800–1000 °C. Films deposited using the Cp-based process started to crystallize at 800 °C while films deposited using the thd-based process still remained amorphous at this temperature. All films became polycrystalline after annealing at 1000 °C. The properties of the amorphous films were very promising for applications as the films were smooth and they exhibited high permittivity (14–16) and low leakage current.
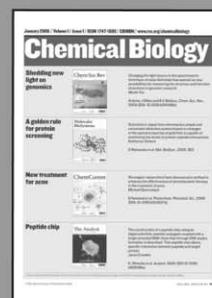
Acknowledgements

References

1 J. Päiväsaari, J. Niinistö, P. Myllymäki, C. L. Dezelah, IV, C. H. Winter, M. Putkonen, M. Nieminen and L. Niinistö, *Top. Appl. Phys.*, 2006, in press.

2 T. Heeg, M. Wagner, J. Schubert, Ch. Buchal, M. Boese, M. Luysberg, E. Cicerrella and J. L. Freeouf, *Microelectron. Eng.*, 2005, **80**, 150.

3 M. Leskelä and M. Ritala, *J. Solid State Chem.*, 2003, **171**, 170.

4 C. Zhao, T. Witters, B. Brijs, H. Bender, O. Richard, M. Caymax, T. Heeg, J. Schubert, V. V. Afanas'ev, A. Stesmans and D. G. Schlom, *Appl. Phys. Lett.*, 2005, **86**, 132903.

5 R. D. Shannon and C. T. Prewitt, *Acta Crystallogr., Sect. B*, 1970, **26**, 1046.

6 D. I. Chernobrovkin, I. A. Korzh and M. N. Piganov, *Instrum. Exp. Tech.*, 1976, **19**, 1137.

7 S. A. Kutolin, V. I. Kotyukov, S. N. Komarova and D. I. Chernobrovkin, *Inorg. Mater. (Transl. of Neorg. Mater.)*, 1979, **15**, 615.

8 P. M. Rasulov, Kh. R. Tulyaganov, Z. A. Iskanderova, T. D. Radjabov, M. A. Alimova, L. P. Kovarski and V. A. Krakhmalyov, *Mater. Sci. Eng., A*, 1991, **139**, 372.

9 J. M. Badie and M. Foex, *J. Solid State Chem.*, 1978, **26**, 311.

10 N. V. Porotnikov, K. I. Petrov, V. N. Tsygankov and M. E. Bogdanova, *Inorg. Mater. (Transl. of Neorg. Mater.)*, 1980, **16**, 62.

11 J. B. Clark, P. W. Richter and L. du Toit, *J. Solid State Chem.*, 1978, **23**, 129.

12 I. M. Maister, L. M. Lopato, Z. A. Zaitseva and A. V. Shevchenko, *Inorg. Mater. (Transl. of Neorg. Mater.)*, 1991, **27**, 1997.

13 M. Ritala and M. Leskelä, in *Handbook of Thin Film Materials*, ed. H.S. Nalwa, Academic Press, New York, 2002, vol. 1, pp. 103–159.

14 L. Niinistö, J. Päiväsaari, J. Niinistö, M. Putkonen and M. Nieminen, *Phys. Status Solidi A*, 2004, **201**, 1443.

15 L. Niinistö, M. Ritala and M. Leskelä, *Mater. Sci. Eng., B*, 1996, **B41**, 23.

16 R. L. Puurunen, *J. Appl. Phys.*, 2005, **97**, 121301.

17 M. Putkonen, T. Sajavaara, J. Niinistö, L.-S. Johansson and L. Niinistö, *J. Mater. Chem.*, 2002, **12**, 442.

18 E. Gourba, A. Ringuede, M. Cassir, A. Billard, J. Päiväsaari, J. Niinistö, M. Putkonen and L. Niinistö, *Ionics*, 2003, **9**, 15.

19 M. Vehkamäki, T. Hänninen, M. Ritala, M. Leskelä, T. Sajavaara, E. Rauhala and J. Keinonen, *Chem. Vap. Deposition*, 2001, **7**, 75.

20 A. Kosola, M. Putkonen, L.-S. Johansson and L. Niinistö, *Appl. Surf. Sci.*, 2003, **211**, 102.

21 A. Kosola, J. Päiväsaari, M. Putkonen and L. Niinistö, *Thin Solid Films*, 2005, **479**, 152.

22 H. Seim, H. Mölsä, M. Nieminen, H. Fjellvåg and L. Niinistö, *J. Mater. Chem.*, 1997, **7**, 449.

23 M. Nieminen, T. Sajavaara, E. Rauhala, M. Putkonen and L. Niinistö, *J. Mater. Chem.*, 2001, **11**, 2340.

24 M. Nieminen, S. Lehto and L. Niinistö, *J. Mater. Chem.*, 2001, **11**, 3148.

25 O. Nilsen, M. Peussa, H. Fjellvåg, L. Niinistö and A. Kjekshus, *J. Mater. Chem.*, 1999, **9**, 1781.

26 M. Putkonen, M. Nieminen, J. Niinistö, T. Sajavaara and L. Niinistö, *Chem. Mater.*, 2001, **13**, 4701.

27 H. Mölsä, L. Niinistö and M. Utriainen, *Adv. Mater. Opt. Electron.*, 1997, **4**, 389.

28 M. Putkonen, T. Sajavaara, L.-S. Johansson and L. Niinistö, *Chem. Vap. Deposition*, 2001, **7**, 44.

29 E. P. Gusev, E. Cartier, D. A. Buchanan, M. Gribelyuk, M. Copel, H. Okorn-Schmidt and C. D'Emic, *Microelectron. Eng.*, 2001, **59**, 341.

30 J. Niinistö, M. Putkonen and L. Niinistö, *Chem. Mater.*, 2004, **16**, 2953.

31 J. Päiväsaari, M. Putkonen and L. Niinistö, *Thin Solid Films*, 2005, **472**, 275.
32 K. J. Eisentraut and R. E. Sievers, *J. Am. Chem. Soc.*, 1965, **87**, 5254.
33 M. Ylilammi and T. Ranta-aho, *Thin Solid Films*, 1993, **232**, 56.
34 UniQuant Version 2 User Manual, Omega Data Systems, Veldhoven, Netherlands, 1994.
35 J. Jokinen, J. Keinonen, P. Tikkanen, A. Kuronen, T. Ahlgren and K. Nordlund, *Nucl. Instrum. Methods Phys. Res., Sect. B*, 1996, **119**, 533.
36 M. Putkonen, T. Sajavaara, L. Niinistö and J. Keinonen, *Anal. Bioanal. Chem.*, 2005, **382**, 1791.
37 A. R. Teren, R. Thomas, J. He and P. Ehrhart, *Thin Solid Films*, 2005, **478**, 206.
38 S. Dueñas, H. Castán, H. Carcía, J. Barbolla, K. Kukli, M. Ritala and M. Leskelä, *Thin Solid Films*, 2005, **474**, 222.
39 J. C. Wang, S. H. Chiao, C. L. Lee, T. F. Lei, Y. M. Lin, M. F. Wang, S. C. Chen, C. H. Yu and M. S. Liang, *J. Appl. Phys.*, 2002, **92**, 3936.